it into the first one. ($\mathbf{h}_1$ is the identity operator.) The groupoid **T** is therefore the set of operations which superposes each substructure onto itself (diagonal terms) or onto the other substructure (off-diagonal terms). The superspace group **G** is called the kernel and **H** the hull of the superspace groupoid. The structure analysis can be made within the framework of the present theory if we use the operators in **G** and **H**.

It is possible to classify the structure into two groups of substructures, one of which consists of the second substructure of Hg and part of the first substructure and the other consists of the third substructure of Hg and the remaining part of the first substructure. The two groups are transformed into each other by the glide plane normal to $\mathbf{a}^{*1} - \mathbf{b}^{*1}$ which transforms $\mathbf{a}^{*1}$ into $\mathbf{b}^{*1}$. In the first substructure, each part has a tetragonal lattice but with monoclinic symmetry. These two parts have no common atoms because they are related by the glide plane. We can apply the groupoid theory to these two groups by recognizing the groups as the substructures in the above discussion. The two structure groups have a five-dimensional superspace group with monoclinic symmetry. When the structure factor of the first group $F_0(\mathbf{h}^e)$ and $\mathbf{h}_2 = \{R|\tau\}$ transforming the first part into the second one are considered, the structure factor of the total structure is given by $F(\mathbf{h}^e) = F_0(\mathbf{h}^e) + \exp(2\pi\mathbf{h}^e\tau)F_0(R^{-1}\mathbf{h}^e)$. In the present case, $\mathbf{h}_2$ is the glide plane so that $R^{-1} = R$. Then the diffraction pattern shows the rotational symmetry due to $\mathbf{h}_2$: $F(R\mathbf{h}^e) = \exp(2\pi R\mathbf{h}^e\tau)F(\mathbf{h}^e)$ because $\{R|\tau\}^2 = \{E|\tau + R\tau\} = \{E|0\}$ and therefore $\exp(2\pi R\mathbf{h}^e\tau) = \exp(-2\pi\mathbf{h}^e\tau)$, where $E$ is the identity operator. This ensures orthorhombic diffraction symmetry. Thus, instead of applying the superspace group for the merged Hg substructure, we can use the superspace groupoid as given in a previous paper (Yamamoto & Ishihara, 1988). This shows the applicability of the present theory to all cases.

The author thanks Dr K. Kato and Dr M. Onoda, National Institute for Research in Inorganic Materials, for valuable discussions and for supplying test data in the development of the new version of *REMOS*.

## References

*International Tables for Crystallography* (1983). Vol. A, edited by T. Hahn. Dordrecht: Kluwer Academic Publishers.

Janner, A. & Janssen, T. (1979). *Physica (Utrecht)*, **A99**, 47-76.

Janner, A. & Janssen, T. (1980). *Acta Cryst.* **A36**, 408-415.

Kato, K. (1990). *Acta Cryst.* **B46**, 39-44.

Onoda, M. & Kato, K. (1991). *Acta Cryst.* **B47**, 630-634.

Onoda, M., Kato, K., Gotoh, Y. & Oosawa, Y. (1990). *Acta Cryst.* **B46**, 487-492.

Pouget, J. P., Shirane, G., Hastings, J. M., Heeger, A. J., Miro, N. D. & MacDiarmid, A. G. (1978). *Phys. Rev. B*, **18**, 3645-3656.

Sadanaga, R. & Ohsumi, K. (1979). *Acta Cryst.* **A35**, 115-122.

Smaalen, S. van (1989). *J. Phys. Condens. Mat.* **1**, 2789-2800.

Ukei, K., Yamamoto, A., Watanabe, Y., Shishido, T. & Fukuda, T. (1992). Submitted to *Acta Cryst.*

Wolff, P. M. de (1974). *Acta Cryst.* **A30**, 777-785.

Wolff, P. M. de, Janssen, T. & Janner, A. (1981). *Acta Cryst.* **A37**, 625-636.

Yamamoto, A. (1982*a*). *Acta Cryst.* **A38**, 87-92.

Yamamoto, A. (1982*b*). *Acta Cryst.* **B38**, 1446-1451, 1451-1456.

Yamamoto, A. & Ishihara, K. N. (1988). *Acta Cryst.* **A44**, 707-714.

Yamamoto, A., Janssen, T., Janner, A. & de Wolff, P. M. (1985). *Acta Cryst.* **A41**, 528-530.

Yamamoto, A. & Nakazawa, H. (1981). *Acta Cryst.* **A37**, 838-842.

---

*Acta Cryst.* (1992). **A48**, 483-490

# On Quantitative Relations among Crystal Structures

By H. Burzlaff and W. Rothammel

*Lehrstuhl für Kristallographie, Institut für Angewandte Physik der Universität Erlangen-Nürnberg,*
*Bismarckstrasse* 10, *D*-8520 *Erlangen, Germany*

(*Received* 25 *September* 1991; *accepted* 3 *January* 1992)

*Dedicated to Professor Dr W. Fischer on the occasion of his* 60*th birthday*

## Abstract

A procedure for the quantitative evaluation of structural relationships among crystal structures is introduced based on the concept of mappings represented by pairs of matrices (**A**, **S**). Lattice relationships, symmetry relationships, local atomic deviations and mapping failures are distinguished and for each type of relationship, a figure of merit is constructed. The different figures are combined in a figure of misfit

0108-7673/92/040483-08$06.00

that might be used for the characterization of the structural relation. Some examples are discussed in detail.

## Introduction

The use of relations among crystal structures is very common in the process of crystal structure description: in many cases a new structure is discussed by comparison with a well known structure. This comparison is usually expressed in words, for example, 'particles $A$ form a distorted cubic close sphere packing' or 'half of the octahedral voids in this packing are occupied by particles $B$'.

Many classification concepts that try to arrange the known structures in a systematic way use the relations among the structures as a fundamental principle. Differences in the judgement of relationships lead, however, to different or even contradictory schemes. For example, the definition of families of structures in the textbook of Megaw (1973, p. 282*ff*) is restricted to 'one-to-one correspondence between all their atoms, and between all their interatomic bonds' (this is weakened later) and does not consider the symmetry relations. On the other hand, it was shown by Bärnighausen (1975) that all the examples given in the textbook show, in addition, well defined relations with respect to symmetry. Quite another idea of structural families was developed by Hellner (1966). Starting from very simple point configurations (such as $I$, $P$ or $F$ lattices), the decomposition of the basic configuration under the influence of subgroup relations leads to structural relations that are governed by symmetry and certain topological properties of the connection patterns. Thus, structures additional to those with one-to-one correspondences between the atoms are related to each other. Many other concepts may be found in the literature. One reason for the differences in the judgement of relationships may arise from the fact that there is a lack of quantitative arguments.

A pair of crystal structures may be related in different ways:

(i) they may be related to each other by correspondence or similarities between their translation lattices;

(ii) they may be related by symmetry, for example, they may have the same group or one space group is a subgroup of the other or there is a common subgroup of importance for both of them;

(iii) they may be related to each other by correspondence between their interatomic bonds or they may have the same or similar coordination schemes.

In this paper, a procedure is proposed that allows not only handling of different aspects of relationships in a valid and unique way but also a quantitative evaluation of the relationship. The procedure is based on the concept of mapping.

## Structural descriptors

Before entering into a detailed discussion, it is convenient to summarize the different possibilities for the description of a crystal structure.

(i) A crystal structure may be described by the list of its *formal parameters*, *i.e.* the space group, the lattice parameters, the Wyckoff positions and the atomic parameters if necessary. This description is complete and allows the construction of the structure (using, for example, a computer). The disadvantage of this parameter list is evident: in most cases it does not give any idea about the arrangement of the atoms. Moreover, this description is not unique since different lists of formal parameters are possible for the same structure (see, for example, Parthé & Gelato, 1984, 1985). This is the reason for several proposals of standardized formal descriptions (Lima-de-Faria, Hellner, Liebau, Makovicky & Parthé, 1990).

(ii) To overcome this disadvantage, it is very common to introduce a *local description* to illustrate the type of neighbourhoods for single atoms. This idea leads to the concept of coordination numbers and polyhedra. Strictly, coordinating neighbours are only those closest to the central atom. In many cases, however, it is difficult to decide whether a neighbour belongs to the coordination sphere of a certain atom or not. Different methods have been introduced to fix the coordination number, *e.g.* the principle of the largest gap (Brunner & Schwarzenbach, 1971). Since even this procedure leads to unsatisfying results in some cases, it may be supplemented by additional procedures, such as the construction of Dirichlet domains, *i.e.* the domain of influence, or by the discussion of equipotential faces *etc.*

(iii) Since in most cases the description of local properties is not sufficient to fix the three-dimensional structure, *global descriptors* are added. These descriptors could be, for example, a Laves symbol or a Laves matrix (Laves, 1930), the use of the concept of $n$-connected nets (Wells, 1954, 1955, 1956), the reference to an aristotype (Megaw, 1973, pp. 216, 282) *etc.* It should be emphasized that it is convenient to designate aristotypes by symmetry-related symbols derived from the nomenclature of lattice complexes (Fischer, Burzlaff, Hellner & Donnay, 1973), as discussed below.

The combined use of local and global descriptors allows at least some illustrative representation of a crystal structure.

## The mapping procedure

A (derived) structure 2 is related to a (basic) structure 1 if a pair of matrices $(\mathbf{A}, \mathbf{S})$ map from structure 1 to structure 2; $\mathbf{A}$ is a non-singular $3\times 3$ matrix, $\mathbf{S}$ is a $(3\times 1)$ column matrix. $\mathbf{M}=(\mathbf{A}, \mathbf{S})$ is called the mapping of the relationship. The relationship is regarded as complete only if the mapping takes into account the following three aspects.

(i) *Mapping of the basis*

If $\mathbf{B}_b = (\mathbf{b}_{1b}, \mathbf{b}_{2b}, \mathbf{b}_{3b})$ represents the basis of the basic structure and $\mathbf{B}_d = (\mathbf{b}_{1d}, \mathbf{b}_{2d}, \mathbf{b}_{3d})$ represents the basis of the derived structure, the following relation holds:

$$\begin{aligned} &\text{if } \dot{\mathbf{B}}_b = \mathbf{B}_d\mathbf{A}, \quad \text{then } \mathbf{B}_b \simeq c\dot{\mathbf{B}}_b \\ &\text{and if } \dot{\mathbf{B}}_d = \mathbf{B}_b\mathbf{A}^{-1}, \quad \text{then } \dot{\mathbf{B}}_d \simeq c\mathbf{B}_d, \end{aligned} \tag{1}$$

*i.e.* the image $\dot{\mathbf{B}}_b$ of $\mathbf{B}_d$ should be similar or very close to $\mathbf{B}_b$ and the image $\dot{\mathbf{B}}_d$ of $\mathbf{B}_b$ should be similar or very close to $\mathbf{B}_d$; $c$ is a common scale factor. This relation can be expressed by the aid of the metric tensor $\mathbf{G}$. Making use of the equations

$$\mathbf{G} = (g_{ik}) = (\mathbf{b}_i\mathbf{b}_k) = \mathbf{B}^T\mathbf{B}, \tag{2}$$

the relations

$$\dot{\mathbf{G}}_b = \mathbf{A}^T\mathbf{G}_d\mathbf{A} \quad \text{and} \quad \dot{\mathbf{G}}_d = (\mathbf{A}^{-1})^T\mathbf{G}_b\mathbf{A}^{-1} \tag{3}$$

hold. For the metric tensors and their images, the relations

$$\mathbf{G}_b \simeq c^2\dot{\mathbf{G}}_b \quad \text{and} \quad c^2\mathbf{G}_d \simeq \dot{\mathbf{G}}_d \tag{4}$$

are valid.

(ii) *Mapping of symmetry operations*

A symmetry operation of the basic structure $(\mathbf{R}_b, \mathbf{T}_b)$ can be mapped into an operation $(\dot{\mathbf{R}}_d, \dot{\mathbf{T}}_d)$ described in the basis system of the derived structure

$$(\dot{\mathbf{R}}_d, \dot{\mathbf{T}}_d) = (\mathbf{A}, \mathbf{S})(\mathbf{R}_b, \mathbf{T}_b + \mathbf{L})(\mathbf{A}, \mathbf{S})^{-1} \tag{5}$$

or, in detail,

$$\dot{\mathbf{R}}_d = \mathbf{A}\mathbf{R}_b\mathbf{A}^{-1}, \tag{5a}$$

$$\dot{\mathbf{T}}_d = \mathbf{A}(\mathbf{T}_b + \mathbf{L}) + (\mathbf{E} - \dot{\mathbf{R}}_d)\mathbf{S}. \tag{5b}$$

The column matrix $\mathbf{S}$ contains the fractional components of the shift vector from the origin of the derived unit cell to the origin of the basic unit cell described in the basis of the derived structure. $\mathbf{L}$ contains the (integral) components of those lattice points of the basic structure that lie inside the unit cell of the derived structure. $\mathbf{E}$ is the unit matrix.

Two different possibilities may occur.

(*a*) The set $\{(\mathbf{R}_d, \mathbf{T}_d)\}$ is contained completely in the set $\{(\dot{\mathbf{R}}_d, \dot{\mathbf{T}}_d)\}$, *i.e.* the space group of the derived structure is a subgroup of the space group of the basic structure; the symmetry relationship is a 'Bärnighausen' relationship. This situation is called a symmetry relationship of type I.

(*b*) The set $\{(\mathbf{R}_d, \mathbf{T}_d)\}$ and the set $\{(\dot{\mathbf{R}}_d, \dot{\mathbf{T}}_d)\}$ have only a common subgroup. This situation is called a symmetry relationship of type II.

(iii) *Mapping of atomic positions*

The same mapping $\mathbf{M}$ used for the generation of the images of the basis and the symmetry operations must be used for the mapping of the atomic positions $\mathbf{X}$. The equation

$$\dot{\mathbf{X}}_d = \mathbf{A}(\mathbf{X}_b + \mathbf{L}) + \mathbf{S} \tag{6}$$

produces images of all atoms of the basic structure, and the relationship can only be accepted if $\dot{\mathbf{X}}_d$ and $\mathbf{X}_d$ coincide or are very close together, where $\mathbf{X}_d$ designates the atomic positions in the derived structure. Inverting the mapping direction, images $\dot{\mathbf{X}}_b$ can be derived for all atoms of the derived structure with coordinates $\mathbf{X}_d$,

$$\dot{\mathbf{X}}_b = \mathbf{A}^{-1}(\mathbf{X}_d - \mathbf{S}) - \mathbf{L}. \tag{7}$$

## Quantitative evaluation of a relationship

Following the different aspects of the concept of mapping, four types of relations are distinguished, namely deviations between the lattices, local atomic displacements, mapping errors and symmetry relations of type I or II. For the first three types, figures of merit will be introduced and used for the comparison of different pairs of structures; they can be combined to a total figure of misfit.

### *Deviations of the lattice*

Since the determinant of the metric tensor equals the square of the volume of the unit cell, it is reasonable to determine the scale factor in (4) [defined in (1)] such that the volume of the image unit cell of the basic structure equals the volume of the unit cell of the derived structure. After this, deviations and distortions can be discussed using metric parameters. As linear deviations of the lengths of the basis vectors and/or distortions with respect to the angles between them may occur, it is not convenient to compare the conventional metric parameters. For the sake of homogeneity, Delaunay parameters (Delaunay, 1933) are introduced. The Delaunay base consists of the four vectors

$$\mathbf{b}_1, \mathbf{b}_2, \mathbf{b}_3, \mathbf{b}_4 \quad \text{with} \quad \mathbf{b}_4 = -\mathbf{b}_1 - \mathbf{b}_2 - \mathbf{b}_3. \tag{8}$$

The scalar products among them are called the Delaunay parameters $s_{12}$, $s_{13}$, $s_{14}$, $s_{23}$, $s_{24}$, $s_{34}$. They contain the same information as the elements of the metric tensor:

$$\begin{aligned} s_{12} &= g_{12}; & s_{14} &= -g_{11} - g_{12} - g_{13}; \\ s_{13} &= g_{13}; & s_{24} &= -g_{12} - g_{22} - g_{23}; \\ s_{23} &= g_{23}; & s_{34} &= -g_{13} - g_{23} - g_{33}. \end{aligned} \tag{9}$$

Angular distortions and linear deviations will be taken into account simultaneously by the expression

$$f_{\text{dev}} = [\textstyle\sum |(|\mathbf{s}_{ik}| - c^{-2}|\dot{\mathbf{s}}_{ik}|)|]/\textstyle\sum |\mathbf{s}_{ik}|, \tag{10}$$

Table 1. *List of structures and aristotypes*

| Structure | Space group and origin | Lattice parameters | Coordinates *x* | *y* | *z* | Reference |
|---|---|---|---|---|---|---|
| '*cP*' | $Pm\bar{3}m$<br>$m\bar{3}m$ | $a = 3.000$ | 0 | 0 | 0 | Aristotype |
| '*cI*' | $Im\bar{3}m$<br>$m\bar{3}m$ | $a = 4.000$ | 0 | 0 | 0 | Aristotype |
| '*cF*' | $Fm\bar{3}m$<br>$m\bar{3}m$ | $a = 4.000$ | 0 | 0 | 0 | Aristotype |
| '*hE*' | $P6_3/mmc$<br>$\bar{3}m$ | $a = 3.000$<br>$c = 4.899$ | $\frac{1}{3}$ | $\frac{2}{3}$ | $\frac{1}{4}$ | Aristotype |
| 'Halogen' | $Abma$<br>$2/m$ | $a = 8.936$<br>$b = 6.710$<br>$c = 4.577$ | 0.1098 | 0 | 0.1388 | Aristotype |
| '$cF; \frac{1}{2}\frac{1}{2}\frac{1}{2}\, cF$' | $Fm\bar{3}m$<br>$m\bar{3}m$ | $a = 6.000$ | 0<br>$\frac{1}{2}$ | 0<br>$\frac{1}{2}$ | 0<br>$\frac{1}{2}$ | Aristotype |
| '$hE; P_{112}$' | $P6_3/mmc$<br>$\bar{3}m$ | $a = 4.000$<br>$c = 6.532$ | 0<br>$\frac{1}{3}$ | 0<br>$\frac{2}{3}$ | 0<br>$\frac{1}{4}$ | Aristotype |
| As | $R\bar{3}m$<br>$\bar{3}m$ | $a = 3.7598$<br>$c = 10.5475$ | 0 | 0 | 0.2271 | *J. Appl. Cryst.* (1969), **2**, 30-36 |
| Se | $P3_121$<br>$2_{[110]} \times 3_1$ | $a = 4.3662$<br>$c = 4.9536$ | 0.2254 | 0 | $\frac{1}{3}$ | *J. Appl. Phys.* (1972), **43**, 1432-1436 |
| α-Fe | $Im\bar{3}m$<br>$m\bar{3}m$ | $a = 2.8665$ | 0 | 0 | 0 | *Z. Angew. Phys.* (1967), **23**, 245-249 |
| Cu | $Fm\bar{3}m$<br>$m\bar{3}m$ | $a = 3.6148$ | 0 | 0 | 0 | *Acta Cryst.* (1969), **A25**, 676-682 |
| Mg | $P6_3/mmc$<br>$\bar{3}m$ | $a = 3.2089$<br>$c = 5.2101$ | $\frac{1}{3}$ | $\frac{2}{3}$ | $\frac{1}{4}$ | *J. Phys. Chem. Solids* (1966), **27**, 547-565 |
| $Cl_2$ | $Abma$<br>$2/m$ | $a = 8.26$<br>$b = 6.24$<br>$c = 4.48$ | 0.1021 | 0 | 0.1222 | *Struct. Rep.* (1979), **45**A, 385<br>*Acta Cryst.* (1965), **18**, 568-569 |
| $Br_2$ | $Abma$<br>$2/m$ | $a = 8.765$<br>$b = 6.752$<br>$c = 4.564$ | 0.110 | 0 | 0.140 | *Acta Cryst.* (1959), **12**, 34-35 |
| $I_2$ | $Abma$<br>$2/m$ | $a = 9.784$<br>$b = 7.136$<br>$c = 4.686$ | 0.1174 | 0 | 0.1543 | *Acta Cryst.* (1967), **23**, 90-91 |
| NiAs | $P6_3/mmc$<br>$\bar{3}m$ | $a = 3.169$<br>$c = 5.034$ | 0<br>$\frac{1}{3}$ | 0<br>$\frac{2}{3}$ | 0<br>$\frac{1}{4}$ | *Can. J. Chem.* (1957), **35**, 1205-1215 |
| MnP | $Pbnm$<br>$\bar{1}$ on $112_1$ | $a = 5.917$<br>$b = 5.25$<br>$c = 3.17$ | 0.1965<br>0.5686 | 0.0049<br>0.1878 | $\frac{1}{4}$<br>$\frac{1}{4}$ | *Acta Chem. Scand.* (1962), **16**, 287-292 |
| $TiO_2$ rutile | $P4_2/mnm$<br>$mmm$ | $a = 4.5845$<br>$c = 2.9533$ | 0<br>0.3049 | 0<br>0.3049 | 0<br>0 | *Acta Cryst.* (1975), **B31**, 1981-1982 |
| $TiO_2$ anatase | $I4_1/amd$<br>$\bar{4}m2$ | $a = 3.7842$<br>$c = 9.5146$ | 0<br>0 | 0<br>0 | 0<br>0.2081 | *Z. Kristallogr.* (1972), **136**, 273-281 |
| $Al_2O_3$ corundum | $R\bar{3}c$<br>$\bar{3}m$ | $a = 4.574$<br>$c = 12.99$ | 0<br>0.3064 | 0<br>0 | 0.3523<br>$\frac{1}{4}$ | *Acta Cryst.* (1982), **A38**, 733-739 |

where the sum is taken over all Delaunay parameters of the derived structure. $f_{\text{dev}}$ is called the figure of deviations.

### *Local displacements*

In general, small deviations between the site of an atom of the derived structure and the related image of the basic structure will occur; these displacements might change from atom to atom, so they are local properties. They can be measured by the distance between the atom and its image,

$$d = |\mathbf{X}_d - \dot{\mathbf{X}}_d|. \tag{11}$$

The effect of all local displacements will be taken into account by

$$f_{\text{dis}} = (\textstyle\sum d_i)/(\sum d_{i\text{coor}}). \tag{12}$$

$f_{\text{dis}}$ is called the figure of displacement. The sum includes all atoms in the unit cell of the derived structure; $d_{i\text{coor}}$ designates the shortest coordination distance for the $i$th atom. Only the terms with $d_i \le 0.5 d_{i\text{coor}}$ are included in the sum.

### *Mapping errors*

Even in strongly related structures, the derived structure may contain interstitial or cavity atoms compared with the basic structure. Of course, the value indicating closeness of relationship should be lowered in these cases. For this purpose, a figure of failures, $f_{\text{fail}}$, is introduced,

$$f_{\text{fail}} = (\textstyle\sum n_d + \sum \dot{n}_d)/(N_d + \dot{N}_d). \tag{13}$$

$N_d$ is the number of atoms in the unit cell of the derived structure, $\dot{N}_d$ is the number of image atoms of the basic structure in the unit cell of the derived structure. The sums include all atoms in this cell; $n_d = 1$ if the value for the related $d$ in (11) exceeds $d_{\text{coor}}/2$, $n_d = 0$ otherwise. The first sum takes care of

Table 2. *Structural relations*

| Pairs of structures | Transformation matrices |  |  |  | Symmetry type, index | Figures of relation |  |  |  |
|---|---|---|---|---|---|---|---|---|---|
|  | *A* |  |  | *S* |  | $f_{\text{dev}}$ | $f_{\text{dis}}$ | $f_{\text{fail}}$ | $f_{\text{mis}}$ |
| As | $\frac{1}{3}$ | $\frac{1}{3}$ | $-\frac{2}{3}$ | 0 | (I) |  |  |  |  |
|  | $-\frac{1}{3}$ | $\frac{2}{3}$ | $-\frac{1}{3}$ | 0 |  | 0.154 | 0.074 | 0.000 | 0.216 |
| '*cP*' | $\frac{1}{6}$ | $\frac{1}{6}$ | $\frac{1}{6}$ | $\frac{1}{4}$ | 8 |  |  |  |  |
| Se | $\frac{2}{3}$ | $-\frac{1}{3}$ | $-\frac{1}{3}$ | $-\frac{1}{3}$ | (I) |  |  |  |  |
|  | $\frac{1}{3}$ | $\frac{1}{3}$ | $-\frac{2}{3}$ | $-\frac{1}{3}$ |  | 0.076 | 0.153 | 0.000 | 0.218 |
| '*cP*' | $\frac{1}{3}$ | $\frac{1}{3}$ | $\frac{1}{3}$ | 0 | 24 |  |  |  |  |
| NiAs | 1 | 0 | 0 | 0 | (I) |  |  |  |  |
|  | 0 | 1 | 0 | 0 |  | 0.179 | 0.000 | 0.000 | 0.179 |
| '*hE*; $P_{112}$' | 0 | 0 | 1 | 0 | 1 |  |  |  |  |
| MnP | $-\frac{1}{2}$ | $-\frac{1}{2}$ | 0 | $\frac{1}{4}$ | (I) |  |  |  |  |
|  | 0 | 0 | 1 | $\frac{1}{2}$ |  | 0.062 | 0.114 | 0.000 | 0.169 |
| '*hE*; $P_{112}$' | $\frac{1}{2}$ | $\frac{1}{2}$ | 0 | $\frac{1}{4}$ | 6 |  |  |  |  |
| $Al_2O_3$ | $\frac{1}{3}$ | $-\frac{2}{3}$ | 0 | 0 | (I) |  |  |  |  |
|  | $\frac{2}{3}$ | $-\frac{1}{3}$ | 0 | 0 |  | 0.043 | 0.068 | 0.091 | 0.184 |
| '*hE*; $P_{112}$' | 0 | 0 | $\frac{1}{3}$ | 0 | 6 |  |  |  |  |
| $TiO_2$ rutile | $-\frac{1}{2}$ | $\frac{1}{2}$ | 0 | 0 | (II) |  |  |  |  |
|  | 0 | 0 | 1 | $\frac{1}{2}$ |  | 0.069 | 0.068 | 0.143 | 0.256 |
| '*hE*; $P_{112}$' | $\frac{1}{2}$ | $\frac{1}{2}$ | 0 | 0 | 6 |  |  |  |  |
| $TiO_2$ anatase | 1 | 0 | 0 | 0 | (I) |  |  |  |  |
|  | 0 | 1 | 0 | 0 |  | 0.239 | 0.076 | 0.143 | 0.398 |
| '*cF*; $\frac{1}{2}\frac{1}{2}\frac{1}{2}$*cF*' | 0 | 0 | $\frac{1}{2}$ | 0 | 12 |  |  |  |  |
| $Cl_2$-'halogen' | 1 | 0 | 0 | 0 | (I) | 0.043 | 0.037 | 0.000 | 0.079 |
| $Br_2$-'halogen' | 0 | 1 | 0 | 0 |  | 0.023 | 0.002 | 0.000 | 0.025 |
| $I_2$-'halogen' | 0 | 0 | 1 | 0 | 1 | 0.047 | 0.040 | 0.000 | 0.085 |
| 'Halogen' | $\frac{1}{2}$ | 0 | 0 | $\frac{1}{8}$ | (I) |  |  |  |  |
|  | 0 | 1 | 0 | 0 |  | 0.347 | 0.210 | 0.000 | 0.484 |
| '*cF*' | 0 | 0 | 1 | $\frac{1}{4}$ | 24 |  |  |  |  |
| '*cF*' | $\frac{1}{2}$ | $\frac{1}{2}$ | 0 | 0 | (II) |  |  |  |  |
|  | $-\frac{1}{2}$ | $\frac{1}{2}$ | 0 | 0 |  | 0.297 | 0.000 | 0.000 | 0.297 |
| '*cI*' | 0 | 0 | 1 | 0 | 3 |  |  |  |  |
| '*hE*' | $-\frac{1}{2}$ | $\frac{1}{2}$ | 1 | $\frac{1}{4}$ | (II) |  |  |  |  |
|  | $\frac{1}{2}$ | $-\frac{1}{2}$ | 1 | $-\frac{1}{4}$ |  | 0.142 | 0.115 | 0.000 | 0.240 |
| '*cI*' | $\frac{1}{2}$ | $\frac{1}{2}$ | 0 | $\frac{1}{4}$ | 12 |  |  |  |  |

missing atoms. Interstitial atoms are taken into account by the second sum; they are identified by reverse mapping.

The three derived figures may be combined in a way similar to obtaining a global figure of merit in direct-methods procedures,

$$f_{\text{mis}} = 1 - (1 - f_{\text{dev}})(1 - f_{\text{dis}})(1 - f_{\text{fail}}). \qquad (14)$$

$f_{\text{mis}}$ is called the figure of misfit. All these figures range between 0 and 1; a relationship is stronger if these figures are closer to 0. Some applications will be discussed below.

### Aristotypes

Before discussing examples, it is necessary to examine more closely the term 'aristotype'. Two kinds of aristotypes may be distinguished:

(i) In agreement with Megaw (1973), an aristotype may be defined as 'the simplest and most symmetric member of any family'. The family consists of all structures that are related to the aristotype in some defined sense. This definition is also in good agreement with the ideas of Ewald & Hermann (1931) concerning an ideal structure ('*Idealfall*'). In addition to maximal simplicitly and highest symmetry, geometrical parameters have to be fixed if they are free (*e.g.* axial ratios in non-cubic structures). To avoid confusion with actual structures, aristotypes of this kind will be designated by symbols derived from the nomenclature of lattice complexes (Fischer *et al.*, 1973) and supplementary geometrical parameters.

(ii) It is not possible to define an aristotype as introduced above for all families of structures. For example, the structures of halogens $Cl_2$, $Br_2$, $I_2$ form a family (Wells, 1975), however, there is no 'simplest and most symmetric' representative. Consequently, no ideal structure is described in the *Strukturbericht* by Hermann, Lohrmann & Philipp (1937). In these cases, it is proposed that the aristotype be fixed by the average of the standardized free parameters and that the aristotype be designated by a trivial name, *e.g.* 'halogen' in the case above.

### Examples

The examples are selected in such a way that structures with strong relationships and structures with poor relationships are included for comparison. Moreover, they are well known to most crystallographers, to give an impression of the validity of the procedure. The structural data for all structures used are presented in Table 1. The table contains the designation of the structure, the space group and information on the origin selected, the lattice parameters, the coordinates and a reference. It starts with the description of seven aristotypes. The symbols '*cP*', '*cI*', '*cF*' designate the three cubic Bravais lattices; '*hE*' designates the hexagonal close packing with the axial ratio $c/a=(24/9)^{1/2}\simeq 1.633$. 'Halogen' means a structure that results from the averages of the parameters of the halogen structures $Cl_2$, $Br_2$, $I_2$. If voids in a basic arrangement (*e.g.* in '*cF*' or '*hE*' *etc.*) are occupied by additional atoms, their distribution is indicated by the symbol following the semicolon: thus '*cF*; $\frac{1}{2}\frac{1}{2}\frac{1}{2}cF$' designates a cubic close packing with occupation of all octahedral voids, '*hE*; $P_{112}$' means a hexagonal close packing with occupation of all octahedral voids. The indices '112' indicate a transformation: the translation vectors $\mathbf{a}'$, $\mathbf{b}'$, $\mathbf{c}'$ of the *P* lattice represented by the octahedral voids must be multiplied by the indices to match the translations of the structural unit cell, *i.e.* $1\mathbf{a}'=\mathbf{a}$, $1\mathbf{b}'=\mathbf{b}$, $2\mathbf{c}'=\mathbf{c}$.

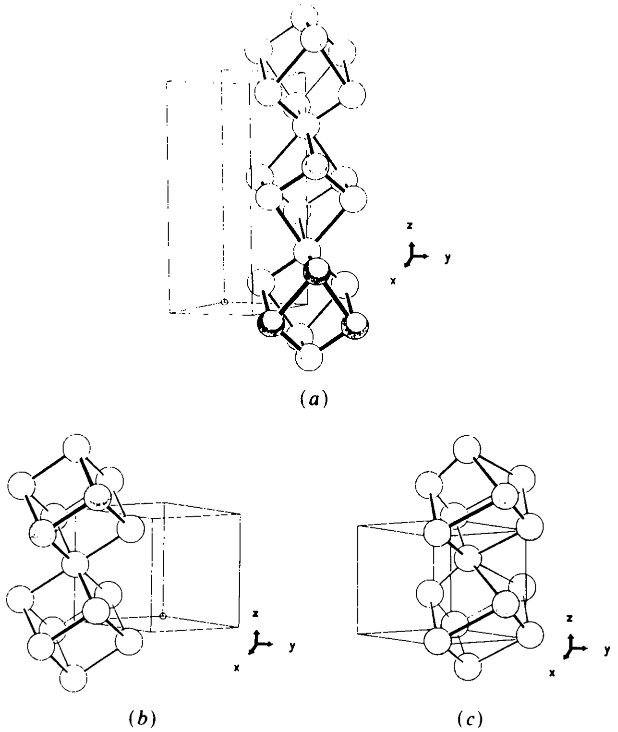

(*a*)

(*b*) (*c*)

Fig. 1. Projections of the structures of (*a*) As, (*b*) '*cP*', (*c*) Se in hexagonal setting.

The results of the quantitative evaluation of the relationships according to the procedure described above are given in Table 2. The first column contains the symbol of the structure and its aristotype. The next two columns give the mapping (**A**, **S**); the following column contains information on the symmetry type and the index of the common subgroup. The last column contains the different figures of merit.

(i) It is well known that the structures of the elements As and Se are strongly related to a cubic *P* lattice (see Fig. 1). The quantitative analysis reveals that the deviations from '*cP*' are of the same magnitude, but the relative importance of the lattice deviations and the local displacements of the atoms is widely different in the two structures.

(ii) The next comparison concerns structures related to the NiAs type (see Figs. 2 and 3). The detailed analysis shows that the deviations of the actual NiAs structure from the aristotype '*hE*; $P_{112}$' are significant because of the lattice deviations; the MnP structure has smaller overall deviations in spite

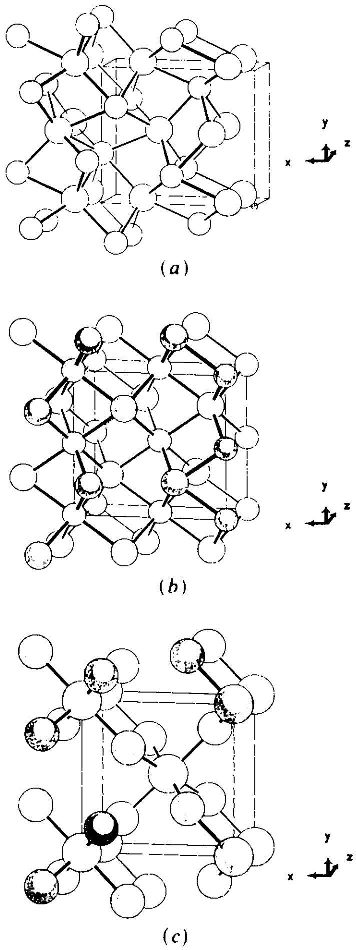

(*a*)

(*b*)

(*c*)

Fig. 2. Projections of the structures of (*a*) MnP, (*b*) '*hE*; $P_{112}$' in orthorhombic setting, (*c*) $TiO_2$ rutile.

of remarkably large local displacements (see Fig. 2*a*, *b*). Even the corundum structure shows a similar figure of misfit although only two-thirds of the octahedral voids are occupied as indicated by the figure of failures. Moreover, the analysis shows that the description for rutile given by Wells (1975) is justified: the main part of the relatively large figure of misfit is due to the half-occupation of the octahedral voids (see Fig. 2*c*).

(iii) The second phase of $TiO_2$, anatase (see Fig. 4), may be regarded as being related to the NaCl structure as already described by Ewald & Hermann (1931). In this case, however, the lattice deviations are substantial and lead, together with the figure of failures, to a large figure of misfit.

(iv) The next example refers to three structures that without any doubt belong to the same aristotype, namely the structures of $Cl_2$, $Br_2$, $I_2$. Consequently, all figures of relation are close to zero. The combined figure of misfit, however, increases to 0.085 in the case of $I_2$.

(v) Although the halogen stucture is clearly a layer structure, it may be regarded as weakly related to a cubic close packing elongated along **b** with tilted unit cells in the direction of **a** (see Fig. 5). The quantitative

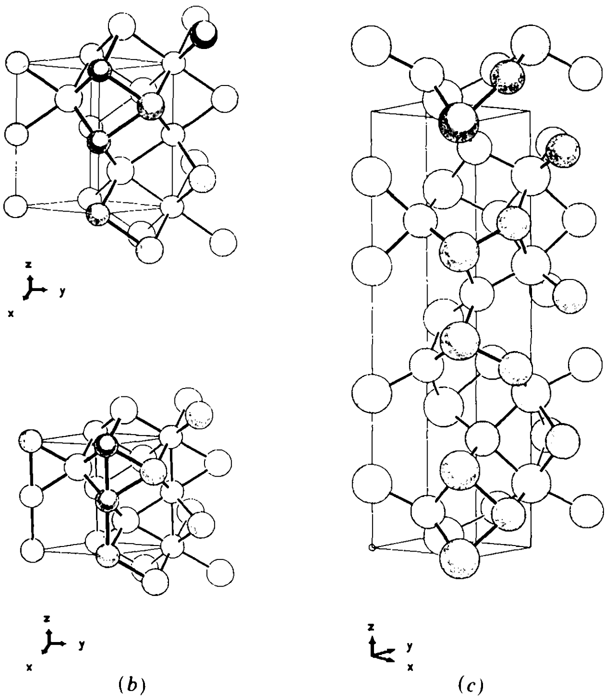

(*b*) (*c*)

Fig. 3. Projections of the structures of (*a*) '*hE*; $P_{112}$' in hexagonal setting, (*b*) NiAs and (*c*) $Al_2O_3$ corundum; for ease of comparison (*c*) shows only parts of the structure.

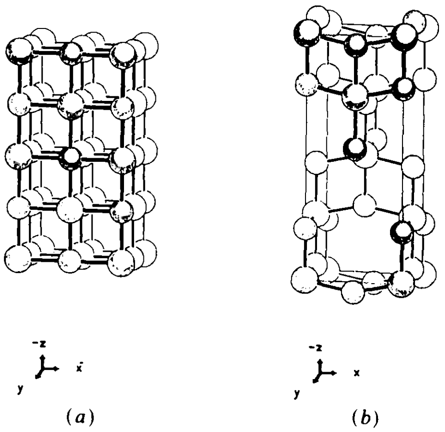

(*a*) (*b*)

Fig. 4. Projections of the structures of (*a*) '*cF*; $\frac{1}{2}\frac{1}{2}\frac{1}{2}$*cF*' and (*b*) $TiO_2$ anatase.

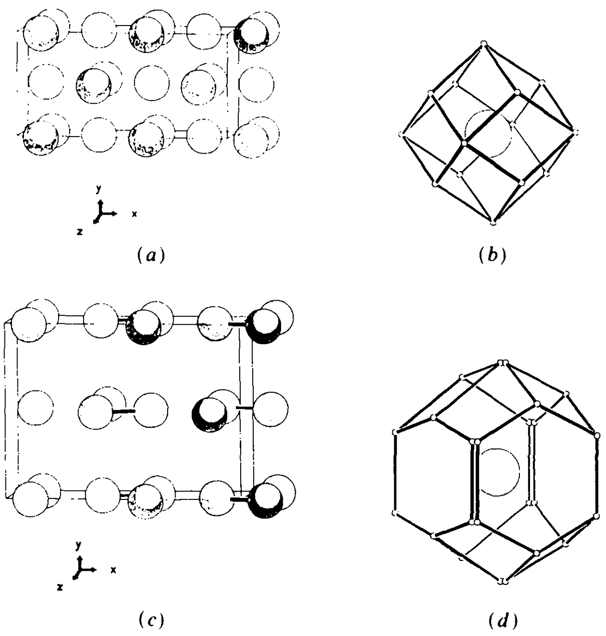

(*a*) (*b*)

(*c*) (*d*)

Fig. 5. Projections of the structure and Dirichlet domain (*a*, *b*) for the cubic close packing '*cF*' and (*c*, *d*) for the aristotype 'halogen'.

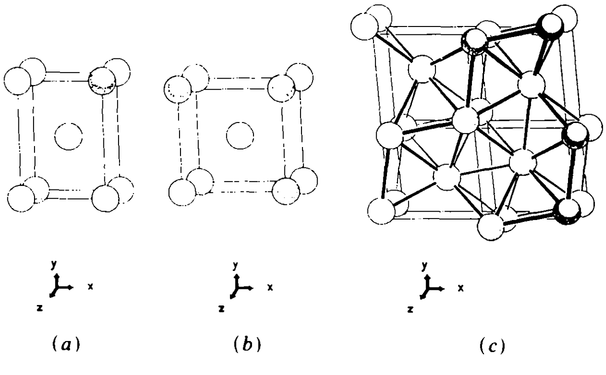

(*a*) (*b*) (*c*)

Fig. 6. Projections of (*a*) '*cF*' in pseudo-*I* setting, (*b*) '*cI*' and (*c*) the hexagonal close packing '*hE*' also in pseudo-*I* setting. It should be recognized that in (*c*) the pseudo-*I* arrangements occur in two different orientations.

evaluation results in a large figure of misfit mostly due to a large figure of deviation stemming from the elongation in the **b** direction. However, the Dirichlet domains support the relation: the rhombi parallel to **b** are changed to hexagons as a consequence of the elongation in the **b** direction, otherwise there are only small changes.

(vi) The last example refers to the relations among the basic arrangements '*cF*', '*cI*', '*hE*', the cubic *I* lattice may be regarded as being between hexagonal close packing and cubic close packing (see Fig. 6). The quantitative evaluation shows that the relation between '*hE*' and '*cI*' is stronger than between '*cF*' and '*cI*'.

### References

BÄRNIGHAUSEN, H. (1975). *Acta Cryst.* **A31**, S3.

BRUNNER, G. O. & SCHWARZENBACH, D. (1971). *Z. Kristallogr.* **133**, 127-133.

DELAUNAY, B. (1933). *Z. Kristallogr.* **84**, 109-149.

EWALD, P. P. & HERMANN, C. (1931). *Strukturbericht* 1913-1928, p. 10.

FISCHER, W., BURZLAFF, H., HELLNER, E. E. & DONNAY, J. D. H. (1973). *Space Group and Lattice Complexes. Natl Bur. Stand. (US) Monogr.* No. 134.

HELLNER, E. E. (1966). *Acta Cryst.* **21**, A252.

HERMANN, C., LOHRMANN, O. & PHILIPP, H. (1937). *Strukturbericht* 1928-1932, p. 5.

LAVES, F. (1930). *Z. Kristallogr.* **73**, 202-265, 275-324.

LIMA-DE-FARIA, J., HELLNER, E., LIEBAU, F., MAKOVICKY, E. & PARTHÉ, E. (1990). *Acta Cryst.* **A46**, 1-11.

MEGAW, H. (1973). *Crystal Structures: a Working Approach.* Philadelphia: W. B. Saunders.

PARTHÉ, E. & GELATO, L. M. (1984). *Acta Cryst.* **A40**, 169-183.

PARTHÉ, E. & GELATO, L. M. (1985). *Acta Cryst.* **A41**, 142-151.

WELLS, A. F. (1954). *Acta Cryst.* **7**, 535-544, 545-554, 842-848, 849-853.

WELLS, A. F. (1955). *Acta Cryst.* **8**, 32-36.

WELLS, A. F. (1956). *Acta Cryst.* **9**, 23-28.

WELLS, A. F. (1975). *Structural Inorganic Chemistry*, 4th ed., p. 329. Oxford: Clarendon Press.

---

*Acta Cryst.* (1992). **A48**, 490-494

# Observed Rocking-Curve Fine Structure on the *Aufhellung* Side of Renninger-Scan Peaks

BY N. G. ALEXANDROPOULOS

*University of Ioannina, GR-45110 Ioannina, Greece and Polytechnic University, Brooklyn, NY 11201, USA*

H. J. JURETSCHKE

*Polytechnic University, Brooklyn, NY 11201, USA*

AND K. T. KOTSIS

*University of Ioannina, GR-45110 Ioannina, Greece*

(*Received 11 July 1991; accepted 7 January 1992*)

## Abstract

Rocking curves of the Si(222) reflection have been measured with $\sigma$-polarized incident radiation in the *Aufhellung* region of a Renninger scan near an $n$-beam interaction point. Even with an angular resolution $\Delta\theta = \pm 8''$, much larger than the intrinsic width of this weak reflection, these curves show a structure with two or more peaks, deviating markedly from that of the standard shape of a (convoluted) weak reflection. Details of the structure vary with the azimuthal angular distance from the interaction point, with the reciprocal-lattice vectors involved in the interaction, and with wavelength. Several typical examples of rocking curves obtained under different experimental conditions are presented and the probable origin and consequences of this structure are discussed.

## Introduction

In the reflecting plane of a two-beam reflection, the intensity is governed by the deviation from the Bragg angle $\Delta\theta$ and by the setting of the azimuthal angle $\varphi$. Rocking curves are obtained by varying $\Delta\theta$ at constant $\varphi$ and are usually independent of $\varphi$, for $\varphi$ far enough from the $n$-beam interaction point. On the other hand, a typical Renninger scan (Renninger, 1937) records the intensity variation of this reflection, integrated over $\Delta\theta$, as a function of azimuthal angle $\varphi$. Such variations occur in the immediate neighbourhood of multiple interaction points, often giving rise to the well known asymmetry which can be used for phase determination (Chang, 1987). The conventional interpretation of the Renninger-scan data assumes that the integration over $\Delta\theta$ is over a standard two-beam line shape. So far, however, experimental

0108-7673/92/040490-05$06.00